



## ECO-FRIENDLY SYNTHESIS OF SILICON NANOPARTICLES FROM BANANA PEEL EXTRACT AND THEIR IN VITRO AND IN VIVO POTENTIAL IN GLIOBLASTOMA TREATMENT

Muhammad Haseeb Ullah<sup>1</sup>, Azka Azhar<sup>1</sup>, Tahir Maqbool<sup>1</sup>, Ali Hamza<sup>1</sup>, Ubaid Ullah Khan<sup>1</sup>,  
Pakeeza Aslam<sup>1</sup>, Barroj Malik<sup>1</sup>, Erum Mubarak<sup>1</sup>, Anam Ghafoor<sup>1</sup>, Mateen Shaukat<sup>2</sup>,  
Ghulam Rasool <sup>1\*</sup>, Abdul Wahab<sup>1\*</sup> and Abdul Razzaq <sup>1,3\*</sup>

<sup>1</sup>Institute of Molecular Biology and Biotechnology, the University of Lahore, Lahore 54000, Pakistan

<sup>2</sup>Faculty of Pharmacy, University of Lahore, Raiwind Road, Lahore, Pakistan

<sup>3</sup>Tropical Crops Genetic Resources Institute, National Key Laboratory for Tropical Crop Breeding, Chinese Academy of Tropical Agricultural Sciences, Haikou 571101, China

\*Corresponding author: [ghulam.rasool@imbb.uol.edu.pk](mailto:ghulam.rasool@imbb.uol.edu.pk) (GR); [wahabgul777@gmail.com](mailto:wahabgul777@gmail.com) (AW);  
[bioformanite@gmail.com](mailto:bioformanite@gmail.com) (AR)

### ABSTRACT

Silicon nanoparticles (SiNPs) have emerged as promising agents in healthcare due to their diverse applications in drug delivery, tissue engineering, regenerative medicine, and cancer therapy. In this study, we developed an eco-friendly, cost-effective method for the biosynthesis of SiNPs using banana peel extract as a natural reducing and stabilizing agent. Banana peels are rich in bioactive compounds, including polyphenols, carotenoids, essential amino acids, dietary fiber, and unsaturated fatty acids, which contribute to nanoparticle formation and stability. The synthesized SiNPs were characterized using a suite of analytical techniques, including X-ray Diffraction (XRD), Fourier Transform Infrared Spectroscopy (FTIR), Ultraviolet–Visible Spectrophotometry (UV-Vis), Scanning Electron Microscopy (SEM), and Energy Dispersive X-ray (EDX) spectroscopy. UV-Vis analysis confirmed the stability and successful formation of SiNPs. The biomedical relevance of these nanoparticles was further explored in the context of glioblastoma multiforme (GBM), one of the most aggressive and prevalent primary brain tumors. Due to their multifunctional capabilities in targeted drug delivery, imaging, and thermal ablation, SiNPs hold significant potential for improving GBM treatment. Moreover, the study highlights elevated p53 expression in glioma tissues, supporting its role as a therapeutic target. This green synthesis approach using banana peels not only provides a sustainable route to nanoparticle production but also offers a novel platform for developing nanotherapeutics against complex diseases such as glioblastoma.

**Keywords:** Green nanotechnology, P53 gene expression, Brain tumor therapeutics, Tumor suppressor biomarkers.

---

Article History (ABR-25-087) || Received: 25 Sep 2025 || Revised: 17 Nov 2025 || Accepted: 29 Nov 2025 || Published Online: 27 Dec 2025

This is an open-access article under the CC BY-NC-ND license (<http://creativecommons.org/licenses/by-nc-nd/4.0/>).

### 1. INTRODUCTION

Scientific research in nanotechnology is expanding rapidly, with diverse applications in manufacturing nanoscale materials (Sharmila et al., 2017). In recent years, nanoparticles (NPs) have gained significant importance across diverse scientific fields, including energy, healthcare, agriculture and environmental sciences, due to their exceptional properties and distinctive characteristics (Karunakaran & Sen, 2011; Aswani et al., 2025). Nature offers insights and methods for creating advanced nanomaterials. According to recent research, biological systems may serve as a "bio-laboratory" to produce nanoscale metal and metal oxide particles using biomimetic techniques (Berger et al., 2022). Environmentally friendly sources of nanoparticles with potential applications have been identified in various organisms, including bacteria, fungi, yeast, plant extracts, and waste products (Sharma et al., 2019). Discrete nanomaterials, nanoscale device materials, and bulk nanomaterials are the three categories of nanoparticles (Rajabi et al., 2019). Discrete nanomaterials, i.e. carbon nanoparticles and nanotubes, have a size range of 1-10nm in at least one dimension and are free-standing. Nanoscale devices or materials are composed of elements that are nanoscale in size, housed within a device, and are themselves nanoscale in size. These are commonly found as thin films on metal oxide. Bulk nanomaterials are discrete nanomaterials or nanoscale materials

---

**Citation:** Ullah MH, Azhar A, Maqbool T, Hamza A, Khan UU, Aslam P, Malik B, Mubarak E, Ghafoor A, Shaukat M, Rasool G, Wahab A and Razzaq A, 2025. Eco-Friendly synthesis of silicon nanoparticles from banana peel extract and their in vitro and in vivo potential in glioblastoma treatment. *Agrobiological Records* 22: 150-162. <https://doi.org/10.47278/journal.abr/2025.057>

that agglomerate and appear as a bulk form while maintaining their nanoscale dimension (Ramesh, 2009).

Banana peels are increasingly recognized as a rich source of natural antioxidants, making them highly suitable for green nanoparticle synthesis. They contain abundant polyphenols, flavonoids, tannins, carotenoids, and vitamins, which act as strong reducing, capping, and stabilizing agents during nanoparticle formation (Ahamed & Khan, 2023). Studies have shown that banana peel extracts exhibit significant antioxidant capacity due to compounds such as gallic acid, catechin, dopamine, and phenolic acids that effectively neutralize free radicals (Raheena & Shankar, 2024). This strong antioxidant profile not only enhances nanoparticle stability but also contributes to improved biocompatibility and reduced cytotoxicity (Lakhani et al., 2025). Previous research demonstrated that banana peel-mediated synthesis of metal and metal oxide nanoparticles results in smaller, more uniform, and functionally active nanostructures compared to chemical methods (Ahamed et al., 2023). Moreover, the abundant phytochemicals in banana peels facilitate rapid electron transfer, accelerating nanoparticle nucleation and growth (Mudrakola et al., 2024). Their low cost, global availability, and high antioxidant content make banana peels an ideal precursor for sustainable nanoparticle development (Liu et al., 2023; Lakhani et al., 2025). Thus, incorporating banana peel extract in SiNP synthesis ensures an eco-friendly, efficient, and biologically potent nanomaterial production platform.

Nanostructured silicon and silica materials show potential for various emerging technologies, such as nano-electronics, photonics, biology, energy harvesting, and storage. Silica nanoparticles (NPs) are particularly beneficial for specific applications (Essien, 2024). These applications include drug delivery, tissue engineering, catalysis, cell imaging, intracellular sensing, and immobilization of enzymes (Nasrollahzadeh et al. 2019). Si-NPs, owing to their distinct characteristics, also hold significant promise in the field of agriculture and could potentially outperform bulk materials in mitigating various abiotic stresses (Cui et al., 2017; Tripathi et al., 2018; Rajiv et al., 2020). Silicon nanoparticles (SiNPs) find extensive use due to their affordability for large-scale production, hydrophobic nature, substantial surface area and pore volume, as well as biocompatibility. Their remarkable adsorption capabilities and non-harmful properties make them stand out in stressful conditions (Simon et al., 2020).

Addressing a spectrum of life-threatening diseases, including chronic conditions like cancer, heart disease, HIV/AIDS, and diabetes, along with severe neurological and infectious diseases, is becoming progressively more complex. Nanomaterials are effectively tackling these challenges by exploring novel avenues for potential treatments, aiming to surpass the limitations of conventional treatment modalities. Nanoparticles promise to impact multiple stages of immune system activation, aimed at cancer. Utilizing nanoparticle-based therapies can instigate the demise of tumor cells, subsequently amplifying the release of neo-antigens from these tumors. Moreover, nanoparticles can be leveraged to enhance antigen presentation and promote the activation of T cells (Joudeh and Linke 2022). Glioblastoma multiforme (GBM) is one of the most frequently diagnosed and highly malignant types of primary brain tumors (Thakkar and Brijesh 2016). The survival rate of patients having glioblastoma is not more than a year (Krętownski et al. 2017). A mutation in the P53 gene is frequently linked to glioblastoma and is associated with poorer outcomes and reduced effectiveness of standard treatments such as chemoradiotherapy. Therefore, targeting P53 could be a promising strategy to enhance the response to these treatments (Lee et al. 2020). Extensive research into novel treatment techniques that selectively target cancer cells is now underway (Huma and Junaid 2024). One of the most recent cancer therapy solutions is the use of nanoparticle-based technology. The current study emphasizes the employment of biosynthesized silicon nanoparticles to evaluate their apoptotic and anticancer potential against glioblastoma cell lines (Alrushaid et al. 2023).

By inducing necrosis or apoptosis in glioblastoma cells, silica nanoparticles (SiNPs) have shown anticancer effects; however, these effects depend on the size and dose of the applied nanoparticles. LN-18 and LBC3 cells' viability was reduced when exposed to different sizes of SiNPs 7nm, 5-15nm, or 10-20nm, at dosages ranging from 12.5 to 1000µg/mL for 24 and 48 hours. When LN-18 and LBC3 cells were treated with 7nm or 10-20nm SiNPs at doses ≥50µg/mL, a strong induction of apoptosis was observed, which is linked to an increase in intracellular reactive oxygen species (ROS) (Shang et al. 2019). The 5-15nm silica nanoparticles (SiNPs) induced strong necrosis without affecting apoptosis in LN-18 glioblastoma cells, unlike their effects on LBC3 cells, due to reduced ROS generation. This highlights that SiNPs' cellular effects vary with exposure conditions, size, dosage, and glioblastoma cell type (Shang et al. 2019). HIF controls the cellular hypoxia response and is implicated in tumor development and angiogenesis. RAFA acts in the MAPK/ERK signaling pathway, stimulating cell proliferation and differentiation. GAPDH, though universally utilized as a housekeeping gene, also plays roles in apoptosis and stress response. AKT3 is a pro-survival signal that is frequently upregulated in cancer, whereas TP53, an established tumor suppressor, regulates cell cycle arrest and apoptosis (Raj et al. 2021). Alterations in the expression of these genes after treatment gave clues about the molecular pathways influenced by the synthesized SANPs. The downregulation of oncogenic markers and upregulation of pro-apoptotic signals that were observed showed that the treatment was successful in derailing important pathways that contribute to cancer cell survival and growth (Majercikova et al. 2022). Green

**Citation:** Ullah MH, Azhar A, Maqbool T, Hamza A, Khan UU, Aslam P, Malik B, Mubarak E, Ghafoor A, Shaukat M, Rasool G, Wahab A and Razaq A, 2025. Eco-Friendly synthesis of silicon nanoparticles from banana peel extract and their in vitro and in vivo potential in glioblastoma treatment. *Agrobiological Records* 22: 150-162. <https://doi.org/10.47278/journal.abr/2025.057>

synthesis of SiO<sub>2</sub> NPs from banana peel and its characterization using different diffraction and microscopy techniques (Mohsin et al. 2020). Evaluate the effect of SiO<sub>2</sub> NPs on the toxicity of the glioblastoma cell line.

## 2. MATERIALS AND METHODS

### 2.1 Preparation of Banana Peel Extract

Banana peels were dried properly at room temperature, then powdered and mixed with 700 mL of distilled water. A quantity of 25g of powder from banana peels was added to distilled water and placed on a string machine at 70°C and 160rpm for 4-5 hours to homogenize it. Filtered it with Whatman filter paper and stored it in a flask.

### 2.2 Synthesis of Silicon Nanoparticles

A solution of 2mM sodium silicate (Na<sub>2</sub>SiO<sub>3</sub>) was mixed with the plant extract at a 1:4 ratio. The solution mixture was kept on a hot plate for 6 hours at 70°C with continuous stirring. The reaction mixture was centrifuged at 7000rpm for 15 minutes after 6 hours of stirring to collect the precipitate/pellet. The obtained pellet was suspended in distilled water and centrifuged 3-4 times to remove impurities. Later, the pellet was dried by pouring it onto a Petri plate and incubated for 24 hours at 37°C. Finally, the obtained SiNPs were powdered well and stored for further analysis and characterization.

### 2.3 Characterization of SiNO<sub>2</sub>

The optical, structural, and morphological features of the biosynthesized SiO<sub>2</sub> nanoparticles were characterized using various characterization tools. Optical properties were investigated using UV-Vis spectrophotometry (model number and company name) with reflectance spectra in the wavelength range of 410–450nm recorded at room temperature. Fourier-Transform Infrared Spectroscopy (FTIR) (model and company name) was performed to determine the chemical bonds and functional groups existing within it, and readings were taken between 4000–515 cm<sup>-1</sup>. The crystalline nature of the nanoparticles was verified by X-ray.

### 2.4 Biological Activity

**2.4.1. Anticancer Activity:** The anticancer activity of SiNPs was measured in the glioblastoma cell line (SF767).

**2.4.2. Cytotoxicity Assay:** The anticancer activity of biosynthesized SiO<sub>2</sub> nanoparticles was tested against the Glioblastoma cell line (SF767). The evaluation of cytotoxicity was done by MTT assay.

**2.4.3. Restoration of Host Cells from Cryopreservation:** Suspended the cryopreserved Glioblastoma SF767 cell line in a water bath at 37°C for defrosting, and subsequently, the cells were diluted by adding 100µL of complete media. Cell suspension was then pipetted out to an Eppendorf tube and centrifuged at 800rpm for 5min. After centrifugation, the supernatant was discarded, and the pellet was resuspended in 200µL of RPMI growth media. The defrosted host cell was placed in the flask containing growth media and incubated at 37°C with 5% CO<sub>2</sub> for 24 hours. Observed the flask under the inverted microscope to see if the cells were attached to the bottom of the flask. The remaining growth medium was drained from the flask and replaced with 7 mL of the new growth medium. The flask was placed in the CO<sub>2</sub> incubator at 37 °C for 48 hours. The flask was observed under the microscope to see the confluent growth of the cells.

**2.4.4. Growth Rate Curve:** According to the established protocols, the Glioblastoma SF767 cell line was maintained in complete media (RPMI with 10% Fetal Bovine Serum (FBS) and 1% Penicillin/Streptomycin (Pen-Strep). During subculture phases, cell viability was counted through Trypan Blue exclusion test using a hemacytometer. This approach favors maintaining the cell growth timelines and cell survival. The Glioblastoma cells with a density of 5 X 10<sup>4</sup> were seeded in 5 Petri dishes of 60 mm. One of the 5 petri dishes was removed from the incubator after 24 hours intervals and cells were counted

**2.4.5. Sub Culturing of Host Cell/ Splitting:** The 80% confluent cells in a T25 flask were subcultured. The media was aspirated from the flask, and 2mL PBS was added to wash cells. The PBS was drained, and 3mL of trypsin was added to it. The flask was placed in an incubator for 3 min. tapped the flask slightly and added 3mL of complete media to it. The cells were centrifuged at 4000rpm for 2min. The supernatant was aspirated, and resuspended the pellet to 1mL media. The cell counting was performed, and the cells were inoculated into 96-well plates.

**2.4.6. Trypan Blue Exclusion Test (Hemacytometer method):** The Trypan Blue staining test was performed to ensure the homogenous quantity of the cells. During the splitting of cells, they were subjected to centrifugation.

**Citation:** Ullah MH, Azhar A, Maqbool T, Hamza A, Khan UU, Aslam P, Malik B, Mubarak E, Ghafoor A, Shaukat M, Rasool G, Wahab A and Razzaq A, 2025. Eco-Friendly synthesis of silicon nanoparticles from banana peel extract and their in vitro and in vivo potential in glioblastoma treatment. *Agrobiological Records* 22: 150-162. <https://doi.org/10.47278/journal.abr/2025.057>

After centrifugation, cells were suspended in RPMI and thoroughly titrated. 95% ethanol was used to clean the hemacytometer and to cover the viewing grid; a 20mm glass coverslip was used. A 100 $\mu$ L of the cell suspension was added to 100 $\mu$ L Trypan Blue stain in a 1.5mL Eppendorf tube and thoroughly titrated. This ratio provided a dilution factor of 2. Approximately 10 $\mu$ L of this suspension was loaded into the grid channel. Viable cells appeared white, and dead cells appeared blue. Cells per 1mL of media = dilution factor x number of cells counted / total area counted x 10,000

**2.4.7. MTT Assay:** Double serial dilutions of sample nanoparticles were made up to 9<sup>th</sup> column of the 96-well plate and 10<sup>th</sup> column had Cells + DMSO. The 11<sup>th</sup> column contained only cells, while DMSO was added to the 12<sup>th</sup> column. After incubation of cells with nanoparticles, 100 $\mu$ L of MTT dye was added to each well and incubated for 4 hours at 37°C with 5% CO<sub>2</sub>. The media was carefully removed from each well without damaging the crystals. A 100 $\mu$ L of DMSO was added to each well to solubilize the crystals. The plate was placed in an incubator for 15 min at 37°C. The Reading of the plate was taken in a plate reader at 520nm. The percentage cell viability was calculated using the following formula:

%Cell viability = absorbance of sample – mean absorbance –  
ve control Mean absorbance +ve control

**2.4.8. Gene Expression through Quantitative Real-Time PCR:** Quantitative PCR (qPCR) was performed to measure the differential expression of genes *HIF*, *RAFA*, *GAPDH*, *AKT3*, and *TP53*.

## 2.5. In Vivo Study

**2.5.1. Animal Model:** Albino Wistar rats (8-10 weeks old, 200-250g) were used in this study. Obtained from the rats were obtained from the animal house of the Institute of Molecular Biology and Biotechnology, The University of Lahore. All procedures followed were approved, from the ethical guidelines set by The Departmental Ethical Review Committee (DERC) at The University of Lahore.

**2.5.2. Experimental Design:** Rats were divided into six groups (n=4 per group) as follows:

- **Group 1:** Normal control (saline treatment)
- **Group 2:** Disease control (AlCl<sub>3</sub>-induced brain cancer)
- **Group 3:** Standard group (AlCl<sub>3</sub>-induced, treated with Temozolomide)
- **Group 4:** Treated 5mg/brain (AlCl<sub>3</sub>-induced, treated with 5mg SiO<sub>2</sub> nanoparticles)
- **Group 5:** Treated 10mg/brain (AlCl<sub>3</sub>-induced, treated with 10mg SiO<sub>2</sub> nanoparticles)
- **Group 6:** Treated 15mg/brain (AlCl<sub>3</sub>-induced, treated with 15mg SiO<sub>2</sub> nanoparticles)

**2.5.3. Treatment Administration:** SiO<sub>2</sub> nanoparticles were administered intravenously via the intraperitoneal route twice a week for 4 weeks. Disease induction was achieved via oral gavage of AlCl<sub>3</sub> for 4 weeks.

**2.5.4. Hematological and Biochemical Analysis:** Blood samples were collected via heart puncture post-treatment for hematological (RBC, WBC, hemoglobin, platelets) and biochemical analyses (liver and renal function, CA 125 levels). The rerum ALT, AST, bilirubin, ALP, creatinine, and urea tests were performed for toxicity.

**2.5.5. Histological Analysis:** After euthanasia, brain tissues were fixed in formalin, sectioned (5 $\mu$ m), and stained with Hematoxylin and Eosin (H&E). Tumor size, necrosis, inflammation, and cellularity were analyzed.

## 2.6. Statistical Analysis

Data was analyzed using appropriate statistical tests (name of test mention here) to compare the differences between experimental groups. Statistical significance will be set at p < 0.05.

## 3. RESULTS

### 3.1. UV-vis Spectrophotometry

The reduction of silicon using banana peel extract to form silicon dioxide nanoparticles (SiO<sub>2</sub> NPs) was confirmed through spectroscopy. The electrons in the conduction bands oscillated due to surface plasmon resonance (SPR). An SPR peak observed between 280nm and 300nm confirmed the formation of SiO<sub>2</sub> NPs after 24 hours of incubation (Fig. 1). The bioactive compounds in the banana peel extract initially reduce SiO to zero-valent silicon atoms. These zero-valent silicon atoms then facilitate the reduction of remaining Si into SiO<sub>2</sub>, resulting in the formation of cluster structures. The formation of SiO<sub>2</sub> NPs was driven by the reduction of silicon ions by the phytochemicals present in the banana peel extract, including tannins, alkaloids, flavonoids, and terpenoids, which

**Citation:** Ullah MH, Azhar A, Maqbool T, Hamza A, Khan UU, Aslam P, Malik B, Mubarak E, Ghafoor A, Shaukat M, Rasool G, Wahab A and Razaq A, 2025. Eco-Friendly synthesis of silicon nanoparticles from banana peel extract and their in vitro and in vivo potential in glioblastoma treatment. *Agrobiological Records* 22: 150-162. <https://doi.org/10.47278/journal.abr/2025.057>

also acted as stabilizing and capping agents for stable SiO<sub>2</sub> NPs formation. The optical band-gap was calculated by plotting Tauc's equation.

$$ah\nu = k(h\nu - E_g)^n$$

Where (k) is a constant, (hν) represents the photon energy, (E<sub>g</sub>) denotes the energy gap, (n) equals 1/2 for direct transitions, and (n) equals 2 for indirect transitions.

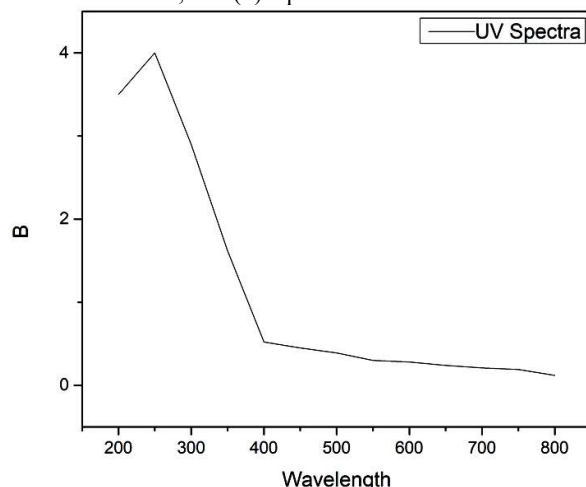


**Fig. 1:** UV-vis spectrophotometry shows a decrease in intensity as the wavelength increases. The highest peak is around 250nm.

cm<sup>-1</sup> and tetrahedral Zn coordination were observed at 857 cm<sup>-1</sup>. The absorption peaks observed in the range of 1238-1080 cm<sup>-1</sup> showed the presence of aliphatic and aromatic amines (C-N) bonds stretching. Presence of N-H and O-H of *Carthamus oxycantha* plant revealed that phenolic compound and proteins bioreduced Zn<sup>+2</sup> into Zn NPs (Fig. 2).

### 3.3. XRD

X-ray diffraction (XRD), as shown in Fig. 3 was employed to analyze the characteristics of the nanoparticles. XRD is a reliable technique for confirming the crystalline nature of the synthesized silica nanoparticles. The XRD pattern of the silica nanoparticles displayed characteristic peaks corresponding to the 101 planes, with diffraction occurring at an angle of 2θ = 20°. The peak width at half maximum is used to evaluate the crystallite size (D) by using the following Debby-Scherrer Formula for SiO<sub>2</sub>, where the size was 38nm observed (Fig. 3).

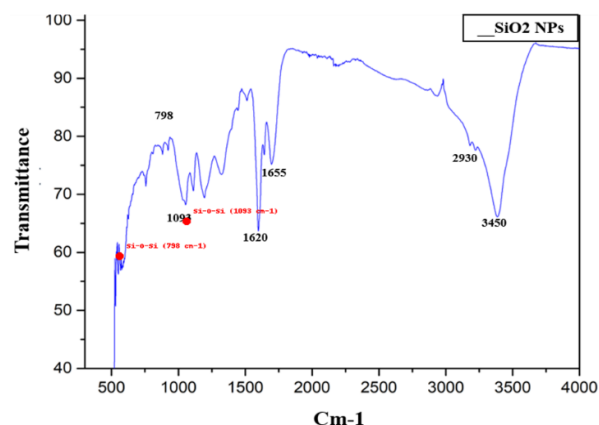


**Fig. 2:** FTIR spectrum shows the presence of Si-O bonds, absorbed water in SiO<sub>2</sub> nanoparticles and hydroxyl groups.

### 3.2. FTIR

The presence of various functional groups (Si-O-Si, O-H, C-H) was identified through Fourier transform infra-red (FTIR) analysis. Absorption band peaks observed at 3394 cm<sup>-1</sup> were corresponded to alcohols, peaks at 1627 cm<sup>-1</sup> were corresponded to aldehydes, amines absorb peaks at 3394.14 cm<sup>-1</sup> and symmetric and asymmetric carboxylate were identified at peaks in range of 1576-120 cm<sup>-1</sup>. The absorption peaks observed at wave number in range of 400-600 cm<sup>-1</sup> showed confirmation of ZnO NPs formation. The peaks for (C=O) observed at 1620 cm<sup>-1</sup>, 574 cm<sup>-1</sup> (O-H) bending and in range between 3400-3450 cm<sup>-1</sup> (O-H) stretching. Peaks observed in the range between 1543-1655 cm<sup>-1</sup> showed the presence of (N-H) bonding of proteins or enzymes contained in extract of *Carthamus oxycantha* plant, Absorption peaks at 2850-2930 cm<sup>-1</sup> corresponded to (C-H) stretching and 1116 cm<sup>-1</sup> (C-H) plane bending. C-O bonding absorption peaks were observed at 1025

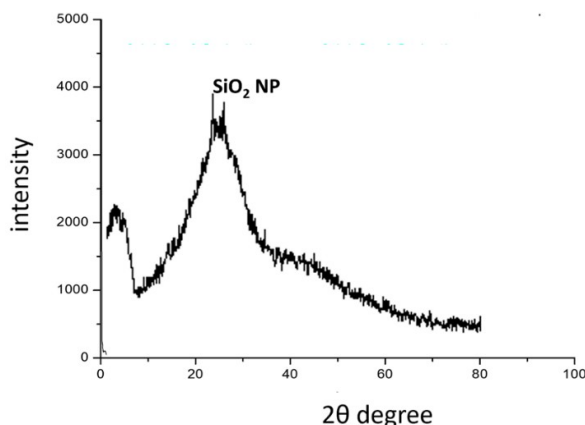


**Fig. 3:** XRD pattern of synthesized SiO<sub>2</sub> nanoparticles (SiO<sub>2</sub> NP). The broad peak centered around 2θ ≈ 22 indicates the amorphous nature of silica nanoparticles.

**Citation:** Ullah MH, Azhar A, Maqbool T, Hamza A, Khan UU, Aslam P, Malik B, Mubarak E, Ghafoor A, Shaukat M, Rasool G, Wahab A and Razzaq A, 2025. Eco-Friendly synthesis of silicon nanoparticles from banana peel extract and their in vitro and in vivo potential in glioblastoma treatment. *Agrobiological Records* 22: 150-162. <https://doi.org/10.47278/journal.abr/2025.057>



### 3.4. SEM and EDX

Silicon nanoparticle size and shape were identified using scanning electron microscopy. Aggregates of silica nanoparticles with spherical shape are seen. The scanning electron microscopy (SEM) analysis revealed that the biosynthesized silicon nanoparticles exhibited various irregular shapes, such as rectangular, radial hexagonal, and spherical forms. To further investigate their surface chemistry, Energy Dispersive X-ray (EDX) spectroscopy was employed. This analysis identified distinct signals for Silicon (Si), along with individual signals for Carbon (C), Oxygen (O), Nitrogen (N), and Phosphorus (P). Additionally, the EDX spectra displayed extra peaks corresponding to Sodium (Na), Potassium (K), and Magnesium (Mg). These extra peaks suggest the presence of phytochemicals from the banana peel leaf extract on the surface of the SiO<sub>2</sub> nanoparticles (Fig. 4).

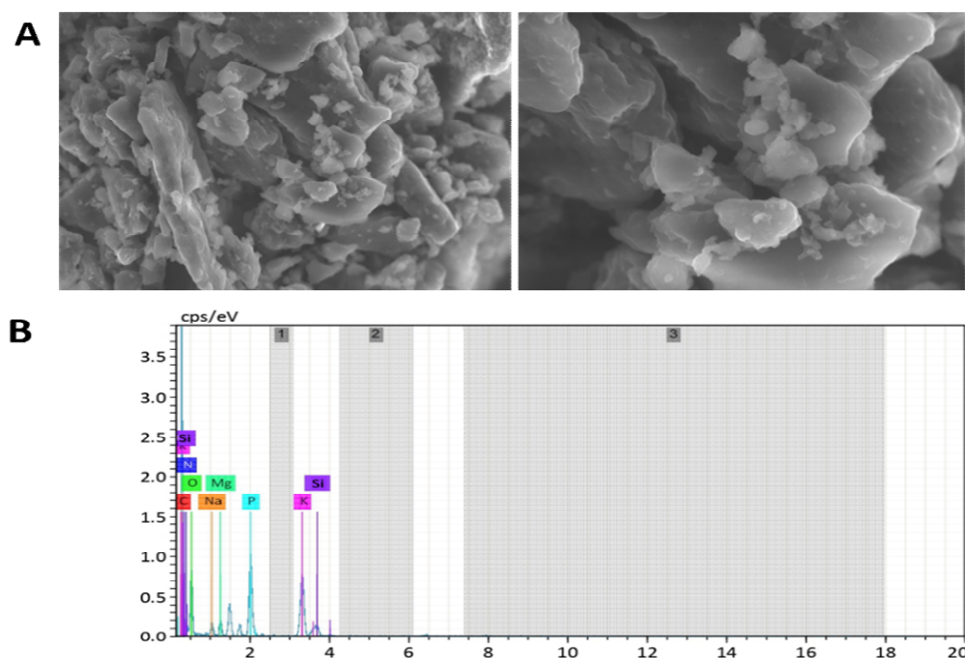


**Fig. 4:** SEM and EDX of SiO<sub>2</sub> NPs.

### 3.5. Biological Activities

**3.5.1. Antifungal Activity:** By using the well diffusion technique, biosynthesized silicone nanoparticles were found to have antifungal activity against *Alternaria alternative*. Three replicates of each silicone nanoparticle concentration (0.25, 0.30, and 0.40mg/mL) were prepared in order to test the antifungal activity. Each concentration was put to PDA medium independently. The lychee fruit's isolated fungus was removed, generating approximately 2-4mm inoculum discs, which were then precisely positioned in the middle of PDA medium plates (Fig. 5). Different concentrations of nanoparticle therapy were applied to the fungus on different PDA media plates under sterile circumstances, and a PDA media plate without nanoparticle treatment functioned as a positive control. After a week of incubation at 26 ± 27 °C, the fungi on these plates shown a variety of growth inhibition at various nanoparticle doses. In all petri plates' growth inhibition was estimated by following formula:

$$\text{Growth inhibition\%} = \frac{(C-T)}{C} \times 100$$

C=Average fungal growth in positive control petri plates.

T=Average fungal growth in NPs treated plates.

**3.5.2. Antibacterial Activity:** The antimicrobial activity of biosynthesized silicon nanoparticles (SiNPs) derived from banana peel extract was evaluated against three bacterial strains: *Staphylococcus*, *E. coli*, and *Bacillus*. The biosynthesized SiNPs demonstrated effectiveness against all tested bacterial strains. The bactericidal effect was notably stronger against Gram-positive bacteria than against Gram-negative bacteria, likely because of their structural differences. The zones of inhibition observed for the biosynthesized SiNPs were 11 mm for *E. coli*, 20 mm for *Bacillus*, and 17 mm for *Staphylococcus* (Fig. 6). These findings are consistent with similar results reported in the literature. The antimicrobial activity of SiNPs were found higher as compared to others, due to the damaging effect of NPs on the microbial membranes by radical formation i.e. oxides or hydroxyl radicals, which destroy

**Citation:** Ullah MH, Azhar A, Maqbool T, Hamza A, Khan UU, Aslam P, Malik B, Mubarak E, Ghafoor A, Shaukat M, Rasool G, Wahab A and Razzaq A, 2025. Eco-Friendly synthesis of silicon nanoparticles from banana peel extract and their in vitro and in vivo potential in glioblastoma treatment. *Agrobiological Records* 22: 150-162. <https://doi.org/10.47278/journal.abr/2025.057>

bacterial membranes.

Additionally, the high surface area of nanoparticles facilitates their penetration through the pores in plasma membranes and interaction with proteins. This increased surface area enhances the contact and friction between the nanoparticles and bacterial cells, leading to a greater uptake of compounds and extracts into microbial cells. It has also been reported that the release of  $H_2O_2$  from the surface of SiNPs is harmful to microbes. The surface area of the SiNPs influences the generation and release of  $H_2O_2$ .  $H_2O_2$  penetrates microbial cells, leading to cell death.

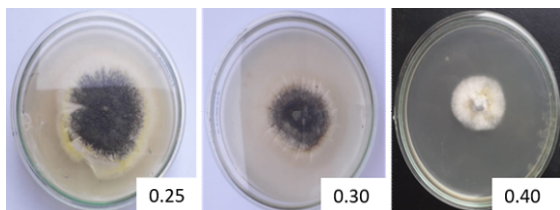


Fig. 5: Antifungal activity.

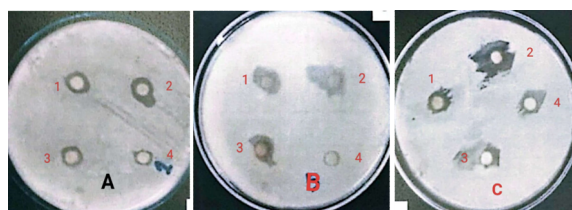


Fig. 6: Antibacterial activity (A) *Staphylococcus*, (B) *E. coli*, (C) *Bacillus*.

**3.5.3. Anti-cancer Activity:** The cytotoxicity of silicon nanoparticles (Si NPs) was analyzed by MTT assay, and their activity was found to be dose-dependent. The cytotoxic activity was highest among the tested concentration at 40  $\mu\text{g/mL}$ , indicating that this concentration is most effective in inhibiting cell viability. Interestingly, the introduction of DMSO seems to affect the result, suggesting a possible interaction between DMSO and the Si NPs that could either augment or modify their cytotoxic impacts. In addition, in all the tested concentrations, Si NPs had much greater cytotoxicity than the plant peel extract, which underlines the superior performance of Si NPs in glioblastoma cell targeting. These results validate the possibility of Si NPs as an even more effective therapeutic agent than treatments based on natural extracts (Fig. 7).

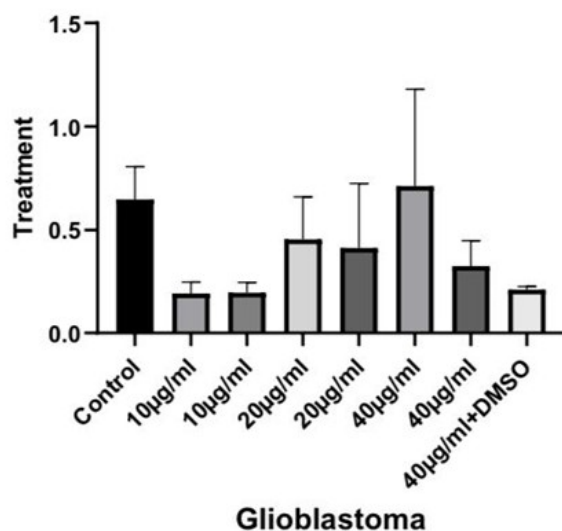


Fig. 7: Anticancer activity of SiO NPs and Peels extract.

decreased TP53 levels, a pivotal tumor suppressor and genomic guardian, suggest compromised DNA damage response and regulation of apoptosis, driving oncogenesis. qPCR analysis further validated that green synthesized SiNPs efficiently downregulated these critical regulators together to suppress tumor cell proliferation and survival through multiple oncogenic signaling axes (Fig. 8).

### 3.6. Comparison of Hematological Parameters across Treatment Groups in Glioblastoma

**3.6.1. Complete Blood Count (CBC) Analysis:** Graphical data demonstrates that the experimental treatment groups, particularly those receiving 10mg and 15mg dosages, significantly improve hematological parameters (WBC, RBC, and hemoglobin) compared to the disease control group. The disease control group exhibited the lowest values

**3.5.4. Gene Expression:** RAFA, the key upstream modulator in the MAPK/ERK signal cascade, contributes importantly to transmitting proliferative and survival signals to cells. Suppressing it contributes to weakened downstream signaling and restricts cancer advancement. BID, a BH3-only BCL-2 family protein, functions as a molecular link between intrinsic and extrinsic apoptotic signals its expression reduction compromises mitochondrial membrane integrity towards favoring apoptosis activation. Downregulation of AKT3, a member of the AKT kinase family, disrupts cancer cell resistance to apoptosis and growth maintenance during stress. Low expression of GAPDH, aside from its traditional function in glycolysis, indicates disruption of energy homeostasis and stress response, and implies generalized impacts on cell viability and metabolism. The reduced expression of HIF, a hypoxia-inducible factor, suggests compromised cellular adaptation to hypoxia an imperative mechanism for tumor survival and metastasis under low-oxygen environments. Finally,

across all parameters, typical of a compromised disease state. The normal control group displayed stable hematological values, while the standard treatment group showed notable improvements over the disease control. Among the experimental treatments, the 15mg dosage resulted in the highest values for all three parameters, surpassing even the standard treatment, suggesting it to be the most effective. These results indicate that the 10mg and 15mg treatments may not only be as effective as the standard treatment but could also offer enhanced therapeutic benefits. Given the importance of hematological parameters in immune function and overall health, these findings suggest that the treatments may improve the body's ability to combat disease, including conditions like glioblastoma. However, further analysis, particularly regarding tumor progression, is necessary to fully evaluate the treatment's effectiveness in glioblastoma (Fig. 9).

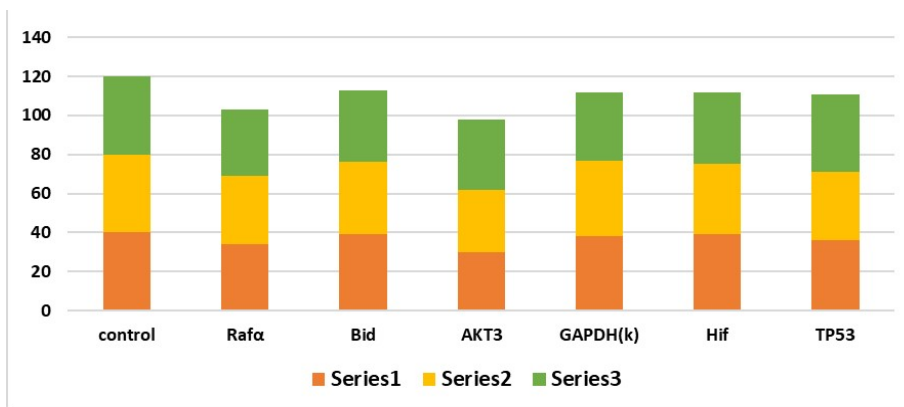


**Fig. 8:** Comparative gene expression levels of control and treated samples.

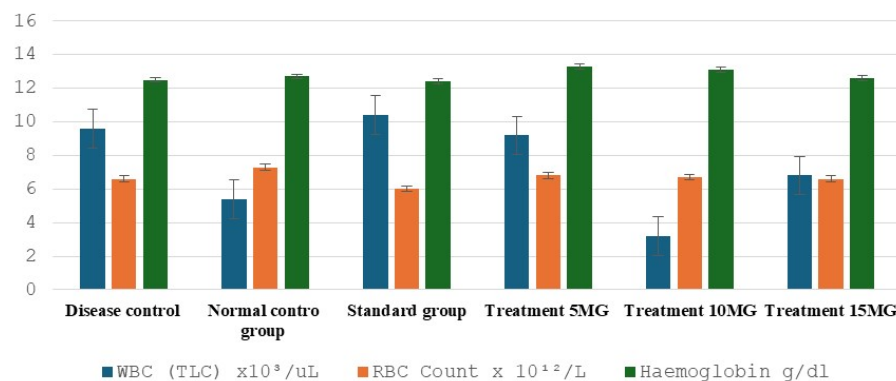


**Fig. 9:** Effect of Different Treatments on Hematological Parameters in Brain Disease Model.

**3.6.2. Liver Function Test (LFT):** Liver function test (LFT) results indicated the experimental treatments (5mg, 10mg and 15mg) only produced very mild elevations in liver enzymes (ALT, AST) compared to the Disease Control and Standard Treatment groups; (Fig. In the Standard Treatment group, ALT and AST were appreciably elevated (ALT 104 U/L and AST 590 U/L), representing exaggerated hepatic insult. In comparison to the control group, the experimental treatments only resulted in mild increases in liver function by Treatment 10mg and 15mg with minimal alterations in ALT and AST. In summary, the experimental treatments in this regimen, particularly at 10mg and 15mg, are lower hepatotoxicity than standard treatment, well-tolerated, and indicate excellent safety and efficacy (Table 1).

**Table 1:** Comparison of LFT Results across Treatment Groups

No.	Group	Bilirubin	ALT (U/L)	AST (U/L)	ALP (U/L)	Total Protein	Albumin
1	Disease control	0.2	31	114	90	8.2	4.5
2	Normal control group	0.5	30	95	115	6.3	3.6
3	Standard group	1	104	590	136	6.5	3.8
4	Treatment 5mg	0.2	50	97	138	7.1	4.1
5	Treatment 10mg	0.2	51	136	141	7.6	4.3
6	Treatment 15mg	0.2	41	146	106	7.1	3.8

**Citation:** Ullah MH, Azhar A, Maqbool T, Hamza A, Khan UU, Aslam P, Malik B, Mubarak E, Ghafoor A, Shaukat M, Rasool G, Wahab A and Razzaq A, 2025. Eco-Friendly synthesis of silicon nanoparticles from banana peel extract and their in vitro and in vivo potential in glioblastoma treatment. *Agrobiological Records* 22: 150-162. <https://doi.org/10.47278/journal.abr/2025.057>



**3.6.3. Renal Function Test (LFT):** Renal function tests RFTs were done to examine the albumin and urea and creatinine levels in different groups to test suitable therapy for renal health. The only significantly higher protein compared to the Disease Control group was albumin, consistent with predictions of changes in protein metabolism with disease state (Table 2). The Normal Control group had much higher urea levels, indicating that they either had higher protein intake or significant

differences in protein metabolism.

**Table 2:** Renal Markers (g/dL) in Control and Treatment Groups

No	Group	Albumin	Urea	Creatinine
1	Disease control	4.5	20	0.4
2	Normal control group	3.6	71	0.4
3	Standard group	3.8	13	0.9
4	Treatment 5mg	4.1	18	0.4
5	Treatment 10mg	4.3	20	0.3
6	Treatment 15mg	3.8	21	0.5

The treatment groups also seemed to trend toward normal/healthy levels of these markers: treatment 10mg was similar to the disease control in urea levels, and treatment 5 and 10mg maintained creatinine levels identical to those of the disease and normal control groups, respectively. While the treatments appear to stabilize kidney function at disease-state levels, this needs in-depth studies to prove efficacy and safety (Fig. 2).

**3.6.4. CA 125 Biomarker:** The graph Fig. 10 shows that Disease Control has the highest CA125 level above normal limits, which is indicative of active disease presence. In the case of the Normal Control group, the CA125 levels fall well within the normal range, indicating the absence of any disease activity. Lower CA125 levels were seen with higher dosage, suggesting a dose-dependency as seen here with the treatment groups (5, 10, and 15mg). However, the 15mg treatment group reaches near-normal control CA125 levels, indicating that the disease may be managed with higher doses of the treatment to levels similar to those seen in normal controls. This trend reinforces the notion that treatment is efficacious against diseases that elevate CA125 levels (Fig. 10).

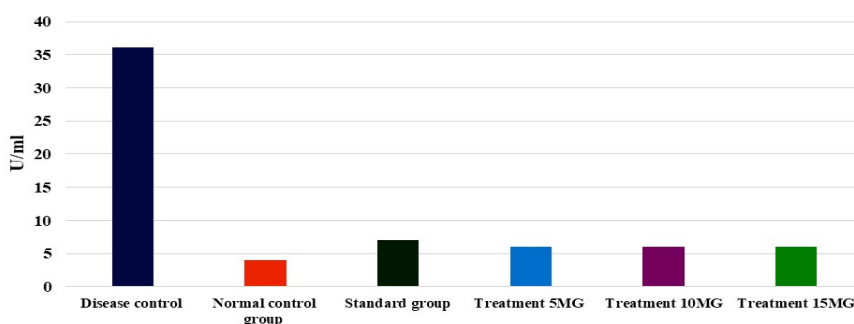


**Fig. 10:** Effect of Treatment Dosage on CA125 Levels (U/mL) in Disease Control versus Normal and Standard Groups.

**3.6.5. Histopathology of Brain:** Histological features of brain tissue show substantial recovery in the treatment groups. The Disease Control group has high-grade neoplasms with karyopyknosis, necrosis, and vacuolations respectively showed severe pathology. On the other hand, the Normal Control group shows healthy tissue. A dose dependent recovery is seen at the higher treatment dosages (10 and 15mg) (Fig. 11) with lower severity of pathological features in comparison to Disease Control. All the giant cells in the 5mg group also show signs of recovery. The Standard group is also showing signs of "recovery phase" features with regions of fibrofatty change and fewer neurodegenerative features further indicating the treatment's efficacy in alleviating brain pathology severity (Fig. 11).

**Table 3:** Spectrophotometer Measurements

Sample #	Concentration (ng/ $\mu$ L)	A260/A280	A260/A230
1	1605.3	1.69	1.99
2	1279.6	1.67	1.85
3	1444.0	1.69	2.04
4	1428.2	1.69	2.11
5	1832.6	1.72	2.13
6	1496.7	1.71	2.11

shows a marked increase in expression of genes when compared to vehicle controls, especially TP53 and GAPDH suggesting that this treatment group evokes a strong response to this treatment dose. The 15mg Treatment Group, however, appears to be less effective than the 10mg group, which could indicate a dosage-dependent effect, since it is still greater than that of the baseline and lower dosages (Fig. 12).

**3.6.7. Genetic Analysis:** Relative gene expression in glioblastoma among treatment groups as illustrated in the graph Normal Group: Heavily expressed genes as a control group. Disease Group levels are also a little higher, suggesting some disease effect. Both the standard drug group and the 5mg treatment group (TG) showed moderate increase in gene expressions raising suggestion of some therapeutic effects. Specifically, the 10mg treatment group

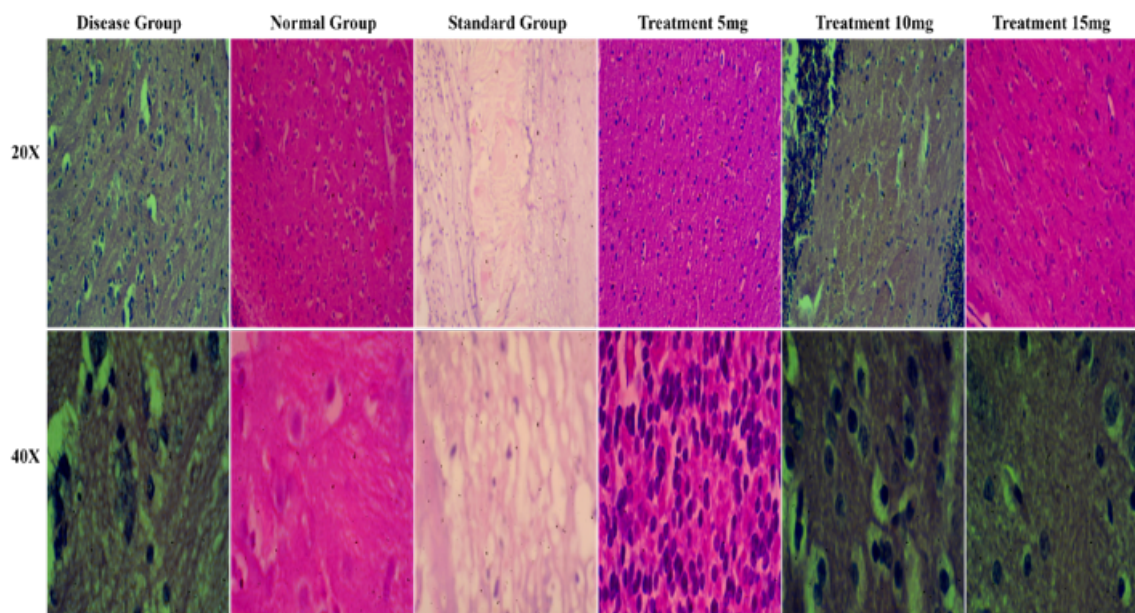


**Fig. 11:** Dose-Dependent Recovery in Brain Tissue Pathology across Treatment Groups.

**3.6.6. Concentration Analysis for cDNA Synthesis:** The spectrophotometric analysis of RNA samples revealed concentrations ranging from 1279.6ng/μL to 1832.6ng/μL. The purity, indicated by A260/A280 ratios, was consistently around 1.69 to 1.72, suggesting good RNA integrity. A260/A230 ratios varied between 1.85 and 2.13, indicating generally acceptable levels of organic contamination (Table 3). These results confirm the suitability of the RNA for subsequent molecular biology applications, such as cDNA synthesis.

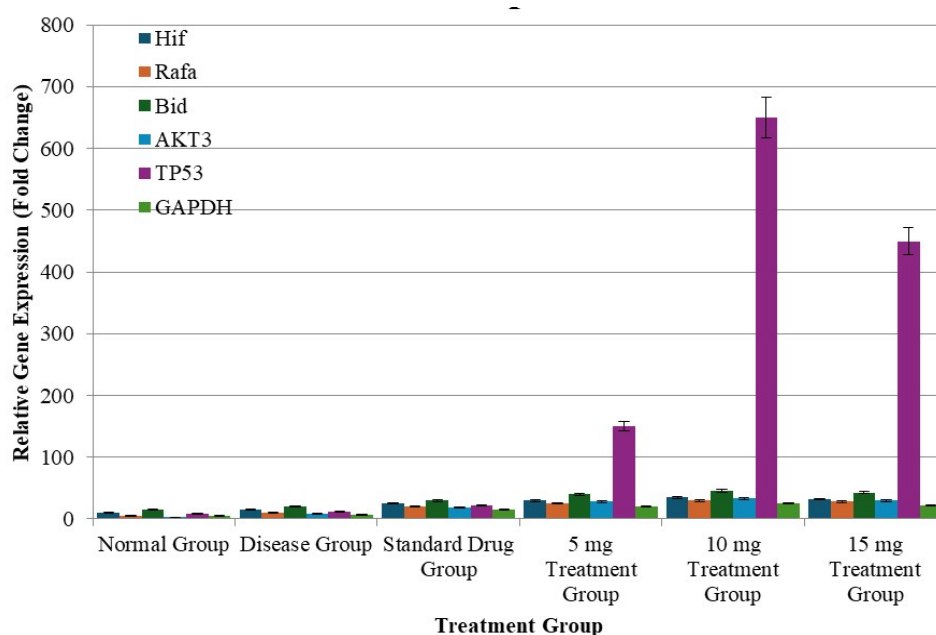


**Fig. 12:** Relative Gene Expression across Treatment Groups.

## 4. DISCUSSION

The present research study demonstrates that eco-friendly biosynthesized silicon nanoparticles (SiNPs), derived from banana peel extract, hold significant promise as therapeutic agents against glioblastoma multiforme (GBM) (Mendiratta et al. 2019). By integrating in vitro and in vivo analyses, this research highlights their anticancer

**Citation:** Ullah MH, Azhar A, Maqbool T, Hamza A, Khan UU, Aslam P, Malik B, Mubarak E, Ghafoor A, Shaukat M, Rasool G, Wahab A and Razzaq A, 2025. Eco-Friendly synthesis of silicon nanoparticles from banana peel extract and their in vitro and in vivo potential in glioblastoma treatment. *Agrobiological Records* 22: 150-162. <https://doi.org/10.47278/journal.abr/2025.057>

efficacy, biocompatibility, and minimal systemic toxicity, thus positioning them as potential alternatives to conventional chemotherapeutic agents. Several key aspects merit deeper discussion: the novelty of the green synthesis approach, the biological mechanisms underpinning the observed effects, the comparative safety and efficacy of SiNPs, and the translational prospects and limitations for GBM therapy (Feng et al. 2023). The use of banana peel extract as a reducing and stabilizing agent for SiNPs synthesis is both innovative and sustainable. Banana peels are an agro-waste product rich in polyphenols, flavonoids, tannins, and amino acids, all of which facilitate nanoparticle formation and stabilization (Liu et al. 2023). This bio-mediated synthesis eliminates the need for toxic chemical reductants or costly synthetic protocols, aligning with the principles of green nanotechnology. Prior reports have shown that plant extracts, fungi, and bacteria can be harnessed for nanoparticle production, but the current study provides new insights into converting food waste into high-value biomedical materials. The dual advantage of waste valorization and therapeutic potential positions this approach as highly relevant for low-cost and sustainable nanomedicine (Wang et al. 2023). The anticancer efficacy of the biosynthesized SiNPs was clearly dose-dependent (Mudrakola et al., 2024), with the strongest cytotoxic effect observed at 40µg/mL in glioblastoma SF767 cells. MTT assays confirmed significant inhibition of cell viability compared to both untreated controls and banana peel extract alone, underscoring the superiority of the nanoparticle formulation. At the mechanistic level, gene expression studies revealed substantial modulation of cancer-associated pathways (Ahamed and Khan 2023).

Notably, SiNP treatment led to the downregulation of oncogenic markers such as AKT3, RAFA, and HIF, which are central to tumor survival, proliferation, and hypoxic adaptation. Concurrently, markers of apoptosis including TP53 were upregulated, reflecting restored tumor-suppressive activity. These findings are consistent with earlier studies where silica nanoparticles induced apoptosis in glioblastoma lines by promoting reactive oxygen species (ROS) generation and mitochondrial dysfunction. However, the current work advances this understanding by demonstrating selective gene-level regulation, suggesting a multi-pronged disruption of oncogenic signaling. The ability of SiNPs to modulate hypoxia-inducible factor (HIF) is particularly important, given that hypoxia drives GBM aggressiveness, angiogenesis, and resistance to therapy glioblastoma (Horta et al. 2025). Similarly, the suppression of RAFA, a critical modulator of MAPK/ERK signaling, weakens proliferative signaling cascades, further impairing tumor progression. Together, these molecular findings corroborate the phenotypic outcomes of reduced viability and highlight the broad therapeutic potential of SiNPs (Zhang et al. 2024).

Animal studies provided further support for the therapeutic potential of SiNPs. Albino Wistar rats treated with SiNPs (10 and 15mg doses) displayed marked improvements in hematological parameters (RBC, WBC, and hemoglobin counts) compared to disease controls, reflecting recovery from tumor-induced systemic compromise. Importantly, SiNP-treated groups also exhibited minimal hepatotoxicity and nephrotoxicity compared with the standard chemotherapeutic agent, Temozolomide, which showed pronounced elevation of liver enzymes. This indicates that SiNPs may achieve therapeutic benefits while minimizing collateral organ damage a key limitation of conventional chemotherapies. Histopathological analysis further reinforced these outcomes. SiNP treatment was associated with significant reductions in necrosis, inflammation, and abnormal cellularity in brain tissues, with higher doses demonstrating near-complete restoration of normal tissue architecture. Such findings highlight the ability of these nanoparticles to cross the blood-brain barrier (BBB), an enduring challenge in GBM therapy. This is consistent with previous reports that nanoscale silicon materials, owing to their size and surface modifications, can traverse the BBB and accumulate selectively in brain tissues (Li et al. 2022). Beyond their anticancer effects, the biosynthesized SiNPs demonstrated robust antibacterial and antifungal activity. This dual bioactivity broadens their potential applications, especially in immunocompromised GBM patients who are highly susceptible to opportunistic infections. The stronger effect observed against Gram-positive bacteria aligns with structural differences in bacterial cell walls, and the role of ROS and hydrogen peroxide release further substantiates their broad-spectrum antimicrobial mechanism. Thus, SiNPs may offer a dual therapeutic advantage by directly targeting tumors while reducing the risk of secondary infections (Zhang et al. 2024).

The therapeutic potential of green-synthesized SiNPs is compelling; however, several considerations must be addressed before clinical translation. First, while in vivo rat models provide proof-of-concept, human GBM is markedly heterogeneous and infiltrative, necessitating extensive validation in orthotopic xenograft or patient-derived tumor models. Second, while gene expression profiling provided mechanistic insights, proteomic and metabolomic studies are required to fully delineate downstream pathways affected by SiNPs. The biodistribution, pharmacokinetics, and long-term safety of SiNPs remain largely unexplored. Although minimal systemic toxicity was observed in this study, chronic administration and cumulative exposure must be assessed to ensure biosafety. Functionalization of SiNPs with targeting ligands such as antibodies or peptides could further enhance tumor specificity while reducing off-target effects. Additionally, combinational strategies pairing SiNPs with established therapies (e.g., Temozolomide or radiotherapy) could yield synergistic benefits and overcome resistance mechanisms.

**Citation:** Ullah MH, Azhar A, Maqbool T, Hamza A, Khan UU, Aslam P, Malik B, Mubarak E, Ghafoor A, Shaukat M, Rasool G, Wahab A and Razzaq A, 2025. Eco-Friendly synthesis of silicon nanoparticles from banana peel extract and their in vitro and in vivo potential in glioblastoma treatment. *Agrobiological Records* 22: 150-162. <https://doi.org/10.47278/journal.abr/2025.057>

## 5. CONCLUSION

The findings of this study suggest that SiO<sub>2</sub> nanoparticles synthesized from banana peel extract hold promise as an effective treatment for glioblastoma. These nanoparticles not only improve P53 gene expression thereby promoting tumour cell apoptosis but also exhibit minimal systemic toxicity making them a safer alternative to the conventional therapies. Although further studies are needed to optimize nanoparticle dosages and evaluate long term effects this research article highlights the potential of nanotechnology in overcoming the challenges associated with treating glioblastoma particularly in targeting the blood-brain barrier. Thus, SiO<sub>2</sub> nanoparticles offer a new direction for developing more effective and sustainable treatments for brain tumors (Glioblastoma).

## Declarations

**Funding:** No funding was available to support the conduct of this study.

**Acknowledgement:** The authors acknowledge the support provided by the Institute of Molecular Biology and Biotechnology, The University of Lahore, Lahore, Pakistan in creating a research environment.

**Conflicts of Interest:** All the authors declare that they have no conflicts of interest regarding this manuscript for authorship, content of the manuscript, and contribution provided by the authors.

**Data Availability:** NA

**Ethics Statement:** Rats are involved in this experimentation and no ethical approval is required. This study follows the 3Rs principle (Replacement, Reduction, Refinement) for animal research, ensuring humane handling and minimal distress. Regular health monitoring and humane euthanasia procedures will be employed if necessary.

**Author's Contributions:** GR-Conceptualization, MHU- preparation of the preliminary draft of the manuscript, AA, BM and AW- review of the manuscript and editing, and MHU- final writing of the manuscript. AH, TM, UUH, AG, EM and PA - Preparation of the first draft of the manuscript, writing the manuscript, revising the manuscript, and MHU5 final editing of the manuscript. GR and AR-Reviewed and approved the final manuscript.

**Generative AI Statements:** The authors declare that no Gen AI/DeepSeek was used in the writing/creation of this manuscript.

**Publisher's Note:** All claims stated in this article are exclusively those of the authors and do not necessarily represent those of their affiliated organizations or those of the publisher, the editors, and the reviewers. Any product that may be evaluated/assessed in this article or claimed by its manufacturer is not guaranteed or endorsed by the publisher/editors.

## REFERENCES

- Aswani, R., Radhakrishnan, E. K., & Visakh, P. M. (2025). Nanoformulations for Agricultural Applications: State-of-the-Art, New Challenges, and Opportunities. *Nanoformulations for Agricultural Applications*, 1-34. <https://doi.org/10.1002/9781119819127.ch1>
- Ahamed, M., & Khan, M. A. M. (2023). Enhanced photocatalytic and anticancer activity of Zn-doped BaTiO<sub>3</sub> nanoparticles prepared through a green approach using banana peel extract. *Catalysts*, 13(6), 985. <https://doi.org/10.3390/catal13060985>
- Alrushaid, N., Khan, F. A., Al-Suhaimi, E. A., & Elaissari, A. (2023). Nanotechnology in cancer diagnosis and treatment. *Pharmaceutics*, 15(3), 1025. <https://doi.org/10.3390/pharmaceutics15031025>
- Berger, T. R., Wen, P. Y., Lang-Orsini, M., & Chukwueke, U. N. (2022). World Health Organization 2021 classification of central nervous system tumors and implications for therapy for adult-type gliomas: A review. *JAMA Oncology*, 8(10), 1493–1501. <https://doi.org/10.1001/jamaoncol.2022.2844>
- Cui, J., Liu, T., Li, F., Yi, J., Liu, C., & Yu, H. (2017). Silica nanoparticles alleviate cadmium toxicity in rice cells: Mechanisms and size effects. *Environmental Pollution*, 228, 363–369. <https://doi.org/10.1016/j.envpol.2017.05.014>
- Essien, N. B. (2024). Rice Husk as Precursor for Silicon Oxide Nanoparticles: Synthesis and Characterization. *Communication In Physical Sciences*, 11(4). <https://doi.org/10.4314/ahsrxrg69>
- Feng, Y., Cao, Y., Singh, R., Janjua, T. I., & Popat, A. (2023). Silica nanoparticles for brain cancer. *Expert Opinion on Drug Delivery*, 20(12), 1749–1767. <https://doi.org/10.1080/17425247.2023.2273830>

**Citation:** Ullah MH, Azhar A, Maqbool T, Hamza A, Khan UU, Aslam P, Malik B, Mubarak E, Ghafoor A, Shaukat M, Rasool G, Wahab A and Razzaq A, 2025. Eco-Friendly synthesis of silicon nanoparticles from banana peel extract and their in vitro and in vivo potential in glioblastoma treatment. *Agrobiological Records* 22: 150-162. <https://doi.org/10.47278/journal.abr/2025.057>



- Horta, M., Soares, P., Pereira, C. L., & Lima, R. T. (2025). Emerging approaches in glioblastoma treatment: Modulating the extracellular matrix through nanotechnology. *Pharmaceutics*, 17(2), 142. <https://doi.org/10.3390/pharmaceutics17020142>
- Huma, Z., & Junaid, M. (2024). The guardian of the genome: P53's role in cancer suppression and therapy. *Baltic Journal of Multidisciplinary Research*, 1(1), 32–39.
- Joudeh, N., & Linke, D. (2022). Nanoparticle classification, physicochemical properties, characterization, and applications: A comprehensive review for biologists. *Journal of Nanobiotechnology*, 20(1), 262. <https://doi.org/10.1186/s12951-022-01477-8>
- Karunakaran, V., & Sen, S. (2011). Biosynthesis of nanoparticles. *International Journal of Pharmaceutical Sciences and Research*, 2, 2781–2785. <https://doi.org/10.1016/j.mtcomm.2024.110741>
- Krętownski, R., Kusaczuk, M., Naumowicz, M., Kotyńska, J., Szyńska, B., & Cechowska-Pasko, M. (2017). The effects of silica nanoparticles on apoptosis and autophagy of glioblastoma cell lines. *Nanomaterials*, 7(8), 230. <https://doi.org/10.3390/nano7080230>
- Lakhani, K. G., Hamid, R., Motamedi, E., & Marviya, G. V. (2025). A review on plant metabolite-mediated nanoparticle synthesis: sustainable applications in horticultural crops. *Frontiers in Nanotechnology*, 7, 1545413. <https://doi.org/10.3389/fnano.2025.1545413>
- Lee, Y.-J., Seo, H. W., Baek, J.-H., Lim, S. H., Hwang, S.-G., & Kim, E. H. (2020). Gene expression profiling of glioblastoma cell lines depending on TP53 status after tumor-treating fields (TTFields) treatment. *Scientific Reports*, 10(1), 12272. <https://doi.org/10.1038/s41598-020-68473-6>
- Li, H., Li, H., Lai, Y., Yang, Z., Yang, Q., Liu, Y., Zheng, Z., Liu, Y., Sun, Y., Zhong, B., Wu, Z., & Guo, X. (2022). Revisiting the preparation progress of nano-structured Si anodes toward industrial application from the perspective of cost and scalability. *Advanced Energy Materials*, 12(7), 2102181. <https://doi.org/10.1002/aenm.202102181>
- Liu, D., Dai, X., Tao, Z., Zhou, H., Hong, W., Qian, H., Cheng, H., & Wang, X. (2023). Advances in blood–brain barrier-crossing nanomedicine for anti-glioma. *Cancer Nanotechnology*, 14(1), 58. <https://doi.org/10.1186/s12645-023-00211-9>
- Majercikova, Z., Dibdiakova, K., Gala, M., Horvath, D., Murin, R., Zoldak, G., & Hatok, J. (2022). Different approaches for the profiling of cancer pathway-related genes in glioblastoma cells. *International Journal of Molecular Sciences*, 23(18), 10883. <https://doi.org/10.3390/ijms231810883>
- Mendiratta, S., Hussein, M., Nasser, H. A., & Ali, A. A. A. (2019). Multidisciplinary role of mesoporous silica nanoparticles in brain regeneration and cancers: From crossing the blood–brain barrier to treatment. *Particle & Particle Systems Characterization*, 36(9), 1900195. <https://doi.org/10.1002/ppsc.201900195>
- Mohsin, M., Jawad, M., Yameen, M. A., Waseem, A., Shah, S. H., & Shaikh, A. J. (2020). An insight into the coating behavior of bimetallic silver and gold core–shell nanoparticles. *Plasmonics*, 15(6), 1599–1612. <https://doi.org/10.1007/s11468-020-01166-y>
- Mudrakola, S. V. S., Koopari, C. L., Kande, R., Rajkumar, K., Anoor, P. K., Burgula, S., & Syed, F. (2024). Synthesis and stabilization of anatase form of biomimetic TiO<sub>2</sub> nanoparticles for enhancing anti-tumor potential. *Green Processing and Synthesis*, 13(1), 20230182. <https://doi.org/10.1515/gps-2023-0182>
- Nasrollahzadeh, M., Sajadi, S. M., Sajjadi, M., & Issaabadi, Z. (2019). Chapter 1 – An introduction to nanotechnology. In M. Nasrollahzadeh, S. M. Sajadi, M. Sajjadi, Z. Issaabadi, & M. Atarod (Eds.), *Interface Science and Technology: Vol. 28. An introduction to green nanotechnology* (pp. 1–27). Elsevier. <https://doi.org/10.1016/B978-0-12-813586-0.00001-8>
- Raheena, S., & Shankar V, S. (2024). A comparative evaluation of the antioxidant property between banana starch-based edible films with and without the inclusion of silicon dioxide nanoparticles. *Interactions*, 245(1), 207. <https://doi.org/10.1007/s10751-024-02060-3>
- Raj, S., Khurana, S., Choudhari, R., Kesari, K. K., Kamal, M. A., Garg, N., Ruokolainen, J., Das, B. C., & Kumar, D. (2021). Specific targeting cancer cells with nanoparticles and drug delivery in cancer therapy. In *Seminars in Cancer Biology* (Vol. 69, pp. 166–177). Elsevier. <https://doi.org/10.1016/j.semcancer.2019.11.002>
- Rajabi, H., Jafari, S. M., Rajabzadeh, G., Sarfarazi, M., & Sedaghati, S. (2019). Chitosan-gum Arabic complex nanocarriers for encapsulation of saffron bioactive components. *Colloids and Surfaces A: Physicochemical and Engineering Aspects*, 578, 123644.
- Rajiv, P., Chen, X., Li, H., Rehaman, S., Vanathi, P., Abd-Elsalam, K. A., & Li, X. (2020). Chapter 18 – Silica-based nanosystems: Their role in sustainable agriculture. In K. A. Abd-Elsalam (Ed.), *Multifunctional hybrid nanomaterials for sustainable agriculture and ecosystems* (pp. 437–459). Elsevier. <https://doi.org/10.1016/B978-0-12-821354-4.00018-2>
- Ramesh, K. T. (2009). *Nanomaterials*. In K. T. Ramesh (Ed.), *Nanomaterials: Mechanics and mechanisms* (pp. 1–20). Springer.
- Shang, Y., Hasan, M. K., Ahammed, G. J., Li, M., Yin, H., & Zhou, J. (2019). Applications of nanotechnology in plant growth and crop protection: A review. *Molecules*, 24(14), 2558. <https://doi.org/10.3390/molecules24142558>
- Sharma, D., Kanchi, S., & Bisetty, K. (2019). Biogenic synthesis of nanoparticles: A review. *Arabian Journal of Chemistry*, 12(8), 3576–3600. <https://doi.org/10.1016/j.arabjoc.2015.11.002>
- Sharmila, G., Fathima, M. F., Haries, S., Geetha, S., Kumar, N. M., & Muthukumaran, C. (2017). Green synthesis, characterization and antibacterial efficacy of palladium nanoparticles synthesized using *Filicium decipiens* leaf extract. *Journal of Molecular Structure*, 1138, 35–40. <https://doi.org/10.1016/j.molstruc.2017.02.097>
- Simon, T., Jackson, E., & Giamas, G. (2020). Breaking through the glioblastoma micro-environment via extracellular vesicles. *Oncogene*, 39(23), 4477–4490. <https://doi.org/10.1038/s41388-020-1308-2>
- Thakkar, M., & Brijesh, S. (2016). Combating malaria with nanotechnology-based targeted and combinatorial drug delivery strategies. *Drug Delivery and Translational Research*, 6(4), 414–425. <https://doi.org/10.1007/s13346-016-0290-2>

**Citation:** Ullah MH, Azhar A, Maqbool T, Hamza A, Khan UU, Aslam P, Malik B, Mubarak E, Ghafoor A, Shaikat M, Rasool G, Wahab A and Razaq A, 2025. Eco-Friendly synthesis of silicon nanoparticles from banana peel extract and their in vitro and in vivo potential in glioblastoma treatment. *Agrobiological Records* 22: 150-162. <https://doi.org/10.47278/journal.abr/2025.057>



- Tripathi, M., Kumar, S., Kumar, A., Tripathi, P., & Kumar, S. (2018). Agro-nanotechnology: A future technology for sustainable agriculture. *International Journal of Current Microbiology and Applied Sciences*, 196–200. <https://doi.org/10.33410/ijcmas/2018/7/3/281604>
- Wang, C., Li, Q., Xiao, J., & Liu, Y. (2023). Nanomedicine-based combination therapies for overcoming temozolomide resistance in glioblastomas. *Cancer Biology & Medicine*, 20(5), 325–343. <https://doi.org/10.20892/j.issn.2095-3941.2022.0761>
- Zhang, J., Zhou, J., Tang, L., Ma, J., Wang, Y., Yang, H., Wang, X., & Fan, W. (2024). Custom-design of multi-stimuli-responsive degradable silica nanoparticles for advanced cancer-specific chemotherapy. *Small*, 20(35), 2400353. <https://doi.org/10.1002/smll.202400353>

---

**Citation:** Ullah MH, Azhar A, Maqbool T, Hamza A, Khan UU, Aslam P, Malik B, Mubarak E, Ghafoor A, Shaukat M, Rasool G, Wahab A and Razzaq A, 2025. Eco-Friendly synthesis of silicon nanoparticles from banana peel extract and their in vitro and in vivo potential in glioblastoma treatment. *Agrobiological Records* 22: 150-162. <https://doi.org/10.47278/journal.abr/2025.057>